Cancer Biol Med 2026. doi: 10.20892/j.issn.2095-3941.2025.0679

ORIGINAL ARTICLE

OPEN ACCESS

# Dietary nitrate drives gastritis by modulating gastric microbiota and metabolites

Lanping Jiang[1]*, Tianhui Li[1]*, Jiayu Wu[1]*, Harry Cheuk Hay Lau[1]*, Chi Chun Wong[1], Xingyu Zhou[1], Alvin Ho Kwan Cheung[2], Qinyao Wei[1], Jing Ren[3], Xiang Zhang[1], Qing Li[1], Yongzhan Nie[4], Jun Yu[1]

[1]Institute of Digestive Disease and Department of Medicine and Therapeutics, State Key Laboratory of Digestive Disease, Li Ka Shing Institute of Health Sciences, The Chinese University of Hong Kong, Hong Kong SAR, China; [2]Department of Anatomical and Cellular Pathology, The Chinese University of Hong Kong, Hong Kong SAR, China; [3]Department of Anaesthesia and Intensive Care and Peter Hung Pain Research Institute, The Chinese University of Hong Kong, Hong Kong SAR, China; [4]Department of Gastroenterology, State Key Laboratory of Holistic Integrative Management of Gastrointestinal Cancers and National Clinical Research Center for Digestive Diseases, Xijing Hospital of Digestive Diseases, Fourth Military Medical University, Xi'an 710032, China

**ABSTRACT**

**Objective:** Dietary nitrate has been increasingly recognized as a potential carcinogen associated with gastritis. In this study the mechanistic role of a high-nitrate diet (NaD) in driving gastritis was elucidated with a focus on modulation of the gastric microbiota composition and metabolomic profiles.

**Methods:** Animals were randomly assigned to two dietary intervention groups using a C57BL/6 mouse model: a NaD containing 7.5% nitrate; or a standard normal diet (ND). Gastric microbiota composition was characterized based on full-length 16S rRNA sequencing and gastric metabolite profiles were analyzed using high-performance liquid chromatography-mass spectrometry (HPLC/MS). Finally, the roles of the microbiome and metabolites in gastritis development were validated using the human gastric epithelial cell line (GES-1), as well as conventional and germ-free mouse models.

**Results:** NaD induced gastritis in conventional mice compared to ND-fed mice. In addition, NaD incited the infiltration of macrophages and neutrophils with elevated levels of inflammatory cytokine genes (*IL-17a*, *Ccl20*, *Cxcl5*, *IL-6*, and *Ccl2*). A significant shift in the composition of the gastric microbiota occurred with an increase in pathogenic bacteria (*Enterococcus gallinarum*, *Prevotella timonensis*, and *Mycobacterium gordona*) and a decrease in probiotics (*Roseburia hominis*, *Clostriduim scindens*, and *Faecalibacterium prausnitzii*). Furthermore, NaD induced alterations in the metabolic profile, marked by an elevated level of 5-hydroxyindoleacetate (5-HIAA), a key downstream metabolite of the tryptophan metabolic pathway. Notably, 5-HIAA also upregulated the levels of inflammatory cytokines in the human gastric epithelial GES-1 cell line. In addition, both *E. gallinarum* colonization and 5-HIAA exposure significantly increased inflammatory responses in conventional and germ-free mouse models.

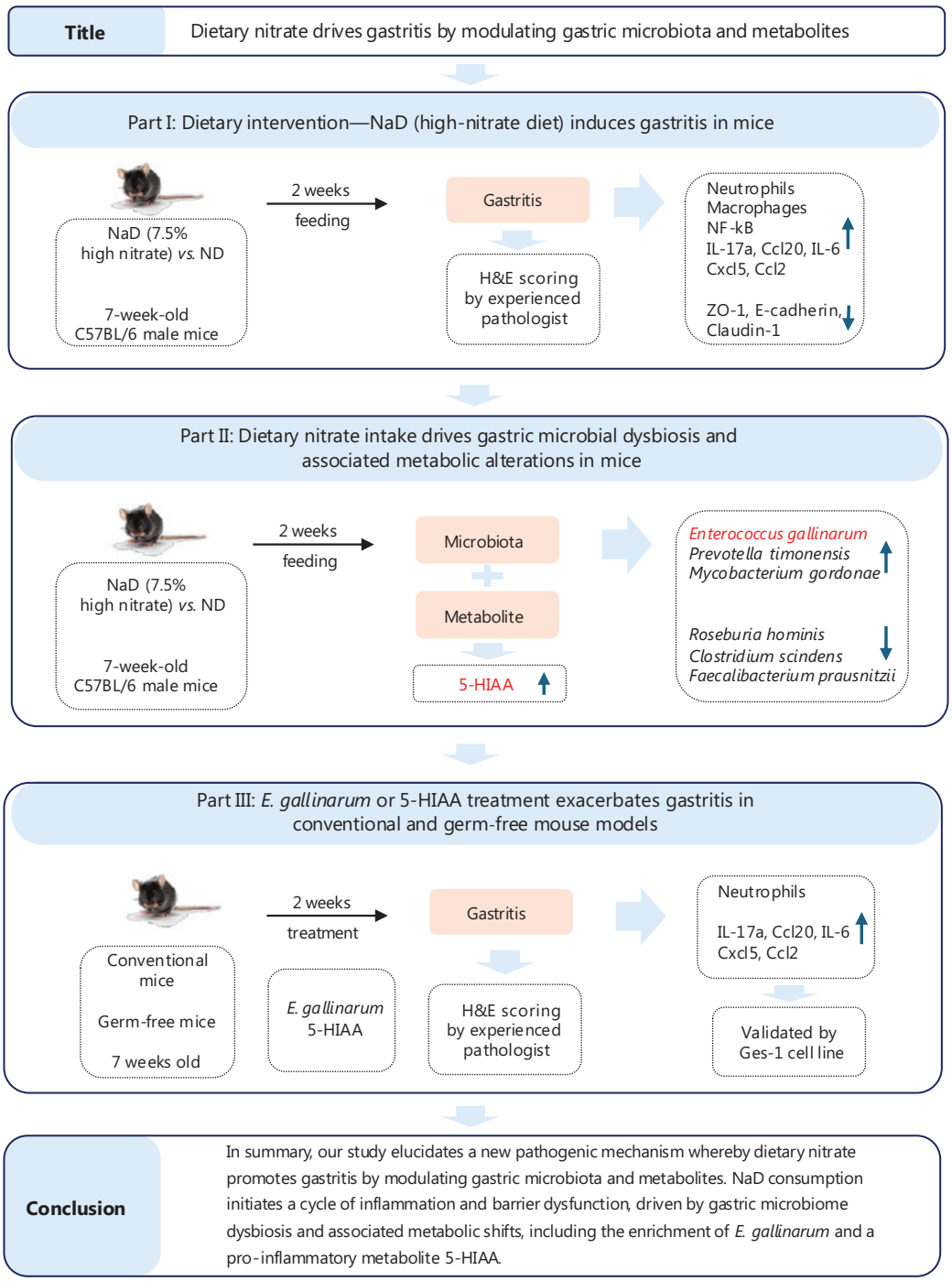
**Conclusions:** NaD drives gastritis in mice by inducing gastric microbial dysbiosis and metabolomic dysregulation with elevated 5-HIAA.

**KEYWORDS** Nitrate diet; gastritis; *Enterococcus gallinarum*; 5-HIAA; germ-free mouse

## Introduction

Chronic gastritis, a common digestive disorder that is characterized by inflammation of the stomach lining, affects > 50% of the global population. Long-term chronic gastritis is a recognized risk factor for the development of gastric cancer (GC)[1,2]. GC is the fifth most common cancer and the third leading cause of cancer-related deaths globally. Indeed, chronic inflammation has been established as a causative factor for GC[3]. Excessive dietary nitrate intake is strongly linked to an elevated risk of GC, in part through a role in promoting gastritis; dietary nitrate is a key precursor to malignant transformation[4,5]. Nitrate is a naturally occurring food constituent and an approved food additive that is often added to processed meats[6]. The consumption of nitrate-rich foods represents the major source of nitrates for the human body. A major part of dietary nitrate exposure (50%–70%) is attributed to the consumption of vegetables, thus reflecting the often-substantial

*These authors contributed equally to this work.
Correspondence to: Jun Yu
E-mail: junyu@cuhk.edu.hk
ORCID ID: https://orcid.org/0000-0001-5008-2153
Received December 11, 2025; accepted February 25, 2026;
published online April 25, 2026.
Available at www.cancerbiomed.org
©2026 The Authors. Creative Commons Attribution-NonCommercial 4.0 International License (CC BY-NC 4.0)




**Study flowchart** (Part I) NaD administration triggers gastritis in mice, characterized by immune cell infiltration, elevated pro-inflammatory cytokines, and impaired gastric mucosal barrier function. (Part II) NaD causes gastric microbial dysbiosis, marked by the enrichment of pathobionts (e.g., *Enterococcus gallinarum*) and depletion of beneficial species with significant reprogramming of the gastric metabolome, including an increase in the tryptophan metabolite, 5-HIAA. (Part III) Functional validation in conventional and germ-free mouse models confirms that *E. gallinarum* colonization or 5-HIAA treatment alone is sufficient to exacerbate gastritis, demonstrating the direct, microbiota-independent roles in driving gastric inflammation. Abbreviations: 5-HIAA, 5-hydroxyindoleacetate; E. gallinarum, Enterococcus gallinarum (*italic); H&E, hematoxylin and eosin; NaD, high-nitrate diet; ND, normal diet.

nitrate content[7]. But the underlying mechanisms between dietary nitrate intake and the development of gastric pathologies have not been established.

Recent metagenomic studies have provided evidence that commensal bacteria, such as Proteobacteria, Firmicutes, Actinobacteria, and Fusobacteria phyla, are regularly detected in gastric mucosa[8]. The ecologic balance of gut microbiota has been increasingly recognized as a critical factor in human health and disease with dysbiosis implicated in the pathogenesis of several diseases[9-11]. Nevertheless, the compositional profiles of gastric microbiota and the potential implication in gastric pathologies has not been sufficiently studied. Our previous study involving the gastric mucosa microbiome across different stages of gastric tumorigenesis underscore the potential importance of oral pathogens (*P. stomatis*, *D. pneumosintes*, *S. exigua*, *P. micra*, and *S. anginosus*) in the progression of GC[12] and experimentally validated *S. anginosus* as the first non-*Helicobacter pylori* bacterial pathogen that promotes gastric tumorigenesis[13]. Reports by others also confirmed that the progression from non-atrophic gastritis to intestinal GC is associated with a shift in the gastric microbiota[14-16]. These findings collectively suggested that the gastric microbiota is an active participant in the pathogenesis of gastric disease. Diet has a major influence on the gut microbiota[17-19]. However, it is unclear how diet might interact with the gastric microbiota to modulate gastric pathologies, such as chronic gastritis and GC.

In this study the role of dietary nitrate in promoting gastritis was investigated. Gastric microbiome alterations induced by a high-nitrate diet (NaD) in mice were then elucidated and the contribution of gut bacterial and metabolites in the development of gastritis was determined. Integrated metagenomic and metabolomic analyses were performed to analyze alterations in the gastric microbiota and metabolites induced by NaD treatment. Studies with NaD-enriched pathogens and metabolites in mouse models confirmed a contributory role in the development of gastritis. The results inferred that NaD promotes gastritis by modulating gastric microbiota and metabolites.

# Materials and methods

## NaD-fed mouse model

Conventional C57BL/6 male mice ($n$ = 40; 7 weeks old) were randomly divided into 3 groups: normal diet (ND); NaD for 1 week (7.5% nitrate diet; **Table S1**); and NaD for 2 weeks. Mice were fed a special customized diet for 1 or 2 weeks. All mice were sacrificed upon completion of the experiments.

## Conventional mouse model

Conventional C57BL/6 male mice ($n$ = 30; 7 weeks old) were randomly assigned to 3 experimental groups: control; *Enterococcus gallinarum (E. gallinarum)* [$1 \times 10^8$ colony-forming units (CFU)]; and 5-hydroxyindoleacetate [5-HIAA] (HY-W008253; MCE, Monmouth Junction, NJ, USA) treatment. Mice in the experimental groups were treated 5 times per week. All mice received an antibiotic cocktail [ampicillin (0.2 g/L), neomycin (0.2 g/L), metronidazole (0.2 g/L), and vancomycin (0.1 g/L)] in drinking water for 1 week prior to microbiota modulation and metabolite administration. All mice were sacrificed upon completion of the experiments.

## Germ-free mouse model

Conventional C57BL/6 male mice ($n$ = 26; 7 weeks old) were randomly assigned to 3 experimental groups: control; *E. gallinarum* ($1 \times 10^8$ CFU); and 5-HIAA treatment. Mice in the experimental groups were treated 5 times per week. All mice were sacrificed upon completion of the experiments.

All animal experiments were performed in accordance with the guidelines of the Animal Experimentation Ethics Committee of The Chinese University of Hong Kong or Germ-free mice platform (AEEC Nos: 21-183-MIS & JTAW20250705-2).

## Bacteria

*E. gallinarum* was isolated from the livers of mice and maintained in our laboratory microbial culture collection for long-term storage.

## Histologic evaluation

The stomachs of mice were excised, cut along the greater curvature, then washed with cold PBS. The non-glandular regions of the stomach were removed and the remaining tissue was cut into fragments, each containing the body and antrum portions of the stomach. Specifically, longitudinal sections were prepared along the greater curvature to include the oxyntic (corpus) and pyloric (antrum) mucosa for histologic assessment, which was consistent with standard protocols for evaluating gastritis. The stomach fragments (approximately 2–3 mm thick) were fixed in freshly prepared 10% formalin solution. Paraffin-embedded gastric tissue sections (5 μm thick) were then cut and stained with hematoxylin and eosin (H&E), and the stained sections were scored by an experienced pathologist.

## Flow cytometry analysis

Mice spleens was harvested for analysis. Tissue samples were suspended in collagenase IV (Sigma-Aldrich, St. Louis, MO, USA) and DNase I (Sigma-Aldrich) and mechanically dissected at 37°C for 30 min with gentle rotation. The digested samples were filtered through 70-μm strainers to obtain single-cell suspensions. Then, the collected cells were washed

with PBS. The cells were incubated with anti-CD16/32 antibody (Biolegend, San Diego, CA, USA) for 10 min at 4°C to block Fc receptors, followed by immunostaining. The cells were incubated at 37°C under 5% $CO_2$ for 3 h and stimulated with a 1:500 cell stimulation cocktail (eBioscience, San Diego, CA, USA). The samples were fixed for intracellular staining using the Foxp3/transcription factor fixation/permeabilization set (eBioscience). The stained samples were analyzed using FACSVerse or FACSCelesta flow cytometers (BD Biosciences, San Jose, CA, USA) and the data were analyzed using FlowJo software (v10.8.1; FlowJo, LLC, Ashland, OR, USA).

## Immunofluorescence (IF) staining

Stomach fragments was fixed in 4% paraformaldehyde overnight at 4°C, then dehydrated with 30% sucrose for 24–48 h. Tissues were permeabilized with 0.1% Triton X-100 (Sigma-Aldrich, St. Louis, MO, USA) in PBS for 5 min, then blocked with 5%–10% normal serum in PBS for 30 min at room temperature. Samples were incubated overnight with primary antibody (F4/80 antibody, MCA497G, Bio-rad, Hercules, California, USA; CD11b antibody, ab133357, Abcam, Cambridge, UK; ZO-1 antibody, 66452-1-Ig, Proteintech, Wuhan, Hubei, China) at 4°C in a humidified chamber, then thrice-rinsed with PBS (5 min each). The samples were incubated with secondary anti-body (Alex Fluor 594 Donkey anti-Rat IgG, A-21209; Alex Fluor 488 Donkey anti-Mouse IgG, A-21202, Thermo Fisher Scientific, Waltham, MA, USA)for 1–2 h at room temperature while protected from light. One drop of mounting medium containing DAPI (Sigma-Aldrich, St. Louis, MO, USA) was applied to the samples. A coverslip was then carefully placed over the samples, avoiding air bubbles. Finally, images were visualized and captured using a fluorescence microscope (DM6000 B; Leica Microsystems, Wetzlar, Germany).

## Immunohistochemistry (IHC) staining

The IHC staining procedure began with deparaffinization and rehydration of the paraffin-embedded tissue sections mounted on microscope slides. An antigen retrieval step was performed as indicated depending on the target antigen, which typically involved heating the slides in a buffer solution. Next, endogenous peroxidase activity was blocked and non-specific binding was minimized by incubating the slides with a blocking buffer (Thermo Fisher Scientific, Waltham, MA, USA). A primary antibody specific (anti-Ly6G; Rabbit, ab238132; Abcam, Cambridge, UK) to the protein of interest was then applied and the slides were incubated overnight at 4°C. After washing, the slides were incubated with a corresponding HRP-conjugated secondary antibody (goat anti-rabbit; Biocare Medical, Pacheco, CA, USA). The enzymatic reaction with a chromogenic substrate, such as DAB (Thermo Fisher Scientific), facilitated visualization of the target protein. The stained sections were then observed and imaged using a light microscope (Leica Microsystems, Wetzlar, Germany).

## PCR array

Total RNA was isolated from the samples using the Trizol reagent (Takara, Kusatsu, Japany). Complementary DNA (cDNA) was synthesized from the extracted RNA using the PrimeScript RT reagent kit (RR037A; Takara). The cDNA was then analyzed using a mouse (PAMM-077Z; Qiagen, Valencia, CA, USA) or human inflammatory response and autoimmunity PCR array (PAHS-077Z; Qiagen).

## Western blot analysis

Protein was extracted with CytoBuster™ Protein Extraction Reagent Simple (71009; Millipore Merck, Burlington, MA, USA) supplemented with proteinase inhibitors (Roche Diagnostics, Basel, Switzerland) and PhosSTOP (Roche). The images were captured and analyzed using Image-Lab software (version 5.2.1; Bio-Rad, Hercules, CA, USA). The levels of protein expression were normalized to the endogenous control, β-actin (#4970; Cell Signaling Technology, Danvers, MA, USA).

## Quantitative PCR

The gastric mucosa total RNA was extracted using the Trizol reagent. The extracted RNA was then reverse-transcribed into cDNA using a PrimeScript RT reagent kit (RR047B; Takara). The resulting cDNA was then analyzed using TB-Green Premix Ex Taq (RR420W; Takara) reagent, which contains SYBR Green dye for fluorescent detection of the amplified target sequences. The resulting cDNA served as the template for the qPCR reaction. The qPCR primers used for validation are listed in **Table S2**.

## Microbiome DNA sequencing and alignment

DNA was extracted from stool, gastric mucosa, and gastric content samples using a DNeasy PowerSoil kit (Qiagen). DNA library preparation and shotgun metagenomic sequencing for the fecal and gastric mucosa samples were performed by Novogene (Tianjin, China) with 43,903,872 ± 2,175,630 (mean ± SD) paired end reads generated (min: 40,761,054; max: 50,681,318). A standard database comprised of 13,844 bacterial genomes from the National Center for Biotechnology Information (Bethesda, MD, USA) was built and the taxonomic profile of the microbiota was obtained using Kraken2 algorithm (v2.0.8-beta; Johns Hopkins University, Baltimore, MD, USA) after host DNA removal and reads quality filtering by KneadData (v0.7.2; Harvard T.H. Chan School of Public Health, Boston, MA, USA). Functional profiling was achieved using HUMAnN2 (v2.8.1; Harvard T.H. Chan School of

Public Health, Boston, MA, USA) with default settings. Full-length 16S rRNA gene amplicon sequences were performed on gastric content or mucosa.

## Microbiome data analysis

Alpha diversity was measured using the Shannon index with R packages vegan (2.6.4; CRAN, Vienna, Austria). Beta diversity was accessed based on the Bray-Curtis distance. Principal coordinates analysis (PCoA) was used for ordination analysis. Community dissimilarities were tested by permutational multivariate analyses of variance (PERMANOVA) with 1000 iterations using the Bray-Curtis distance. This number of iterations was sufficient to determine statistical significance at the $P < 0.05$ level. Bacteria species presented in at least 80% samples and with an abundance > 0.001 were selected for differential abundance analysis with edgeR (3.42.4; Walter and Eliza Hall Institute of Medical Research, Melbourne, VIC, Australia). The Benjamini–Hochberg false-discovery rate (FDR) was used to correct for multiple comparisons and adjusted *P* values < 0.05 were the cut-off.

## Metabolomics profiling

Stool (50 mg), serum (50 μL), gastric mucosa (50 mg), or gastric content samples (50 mg) were subjected to metabolomic profiling (BIOTREE, Shanghai, China). Metabolites were extracted with the proportional addition of cold 80% methanol. After centrifugation at 12,880 × *g* for 15 min at 4°C, the supernatant was collected and analyzed by high-performance liquid chromatography-mass spectrometry using an UHPLC system (Vanquish; Thermo Fisher Scientific, Germering, Germany) with a UPLC HSS T3 column (2.1 mm × 100 mm, 1.8 μm; Thermo Fisher Scientific). An Orbitrap Exploris 120 mass spectrometer (Thermo Fisher Scientific, Bremen, Germany) was used to acquire MS/MS spectra on information-dependent acquisition mode. The acquisition software (Xcalibur; Thermo Fisher Scientific) continuously evaluated the full scan MS spectrum under this mode. The MS raw data were converted to the mzXML format using ProteoWizard (Palo Alto, CA, USA) and the data pretreatment, including peak detection, extraction, alignment, and integration, was achieved by R packages XCMS (V.3.2). An in-house MS2 database was applied in metabolite annotation and the cut-off for annotation was set at 0.3.

## Metabolomics data analysis

Principal component analysis (PCA) was performed to evaluate the overall metabolic composition using the R package, mixOmics, and *P* values was calculated by PERMANOVA with the R package, vegan. Differential metabolite analysis was performed by partial least square discriminant analysis (PLS-DA) and the two-sided Wilcoxon rank-sum test using the R package, mixOmics. The validity of the PLS-DA model was strictly assessed using 6-fold cross-validation to evaluate the predictive capability ($Q^2$) and permutation tests ($n = 1000$; $P < 0.05$) to ensure statistical significance and prevent overfitting. Differential metabolites were identified using a dual-cutoff strategy based on the validated model, as follows: a variable importance in rrojection (VIP) score > 1; and a Benjamini–Hochberg adjusted *P* value < 0.05. Metabolite set enrichment analysis (MSEA) was performed using the online tool, MetaboAnalyst (http://www.metaboanalyst.ca).

## Cell culture

The human normal gastric epithelial cell line, GES-1, was purchased from the Chinese Academy of Sciences (Shanghai, China). All cells were cultured in Dulbecco's modified Eagle's medium [DMEM] (Gibco, Grand Island, NY, USA) with 10% fetal bovine serum [FBS] (Gibco) and 1% penicillin/streptomycin.

## Statistical analysis

All measurements are shown as the mean ± standard deviation. The Mann–Whitney U or Wilcoxon's rank-sum test was used to detect differences in numerical variables and Fisher's exact test was used to evaluate the proportional difference in categorical variables between groups. The associations among metabolites and bacterial species were estimated by Spearman correlation and the *P* value was adjusted by the FDR. All statistical tests were performed with the R Project for Statistical Computing and GraphPad Prism 7.0 (GraphPad, La Jolla, CA, USA). A 2-tailed $P \leq 0.05$ was considered statistically significant. Sample size was determined using G Power 3.1 software (Heinrich Heine University Düsseldorf, Düsseldorf, Germany) based on preliminary data. To detect a large effect size (Cohen's d > 1.5) with a power of 80% and an $\alpha = 0.05$, a minimum of 6 mice per group was needed. Accordingly, 6–10 mice were used for all animal experiments to ensure statistical robustness.

# Results

## NaD induces gastritis in mice with increased infiltration of neutrophils and macrophages

To investigate the effect of NaD administration on the gastric pathologies, Conventional C57BL/6 male mice were fed with a NaD (7.5% $NaNO_3$) or ND for 1 or 2 weeks, respectively (**Figures 1A** and **S1A**). Each mouse exhibited a visibly bloated stomach after 2 weeks of NaD treatment (**Figure S1B**) with a significant increase in the stomach-to-body weight ratio and

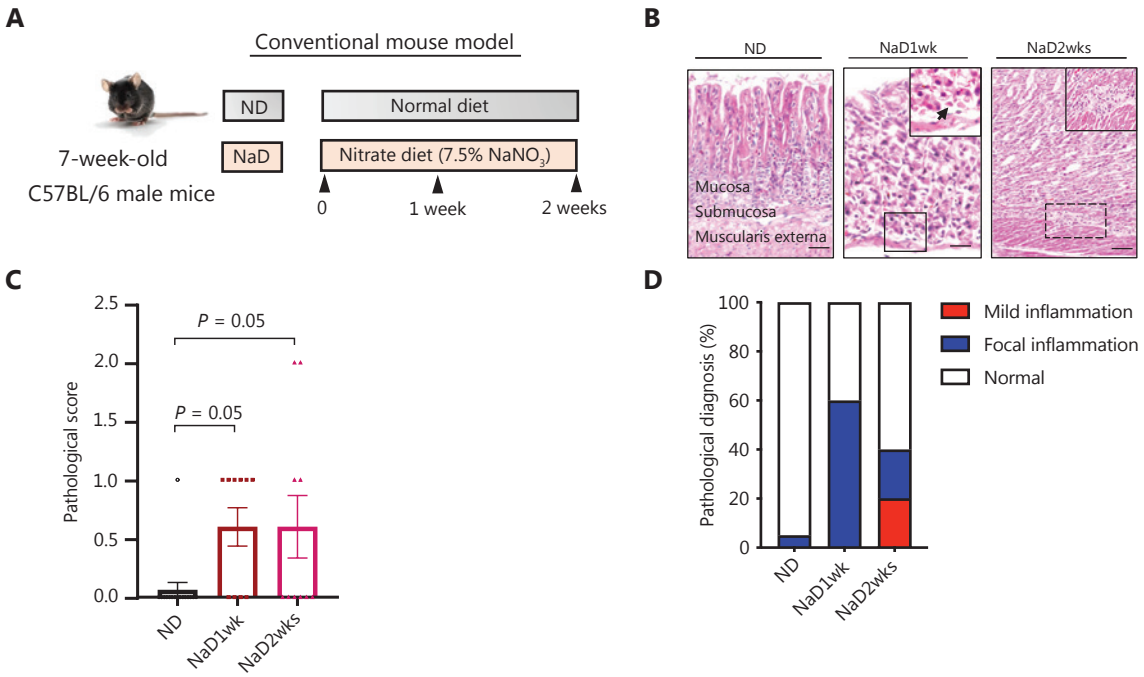



**Figure 1** Continued

stomach volume (**Figure S1C**). Food intake in the NaD treatment groups were decreased compared to the ND treatment groups (**Figure S1D**), which led to weight loss after 2 weeks (**Figure S1E**). The spleen-to-body weight ratio of the NaD-fed mice also increased, suggesting that a NaD may have promoted an inflammatory response. However, the liver-to-body and kidney-to-body weight ratios were unchanged (**Figure S1F**). Importantly, the serum alanine aminotransferase (ALT) and aspartate aminotransferase (AST) levels were comparable between the ND and NaD groups and did not increase, indicating preserved liver function (**Figure S1G**). H&E staining revealed significant immune cell infiltration in the gastric mucosa of the NaD-fed mice (**Figure 1B**), which was associated with significant increase in pathologic scores compared to controls ($P < 0.05$; **Figure 1C**). Accordingly, the levels of focal inflammation were markedly higher in the 1-week NaD group compared to controls; focal and mild inflammation were evident in the 2-week NaD group (**Figure 1D**). IF staining revealed higher infiltration of $CD11b^+F4/80^+$ macrophages and $CD11b^+Ly6G^+$ neutrophils into gastric mucosa after 2-weeks of NaD treatment (**Figure 1E**). The proportion of T lymphocyte subsets were assessed in the spleens of mice from the ND and NaD groups using flow cytometry. A significant decrease in the frequency of $CD3^+$ T cells was noted in the NaD group compared to the ND group ($P = 0.02$). However, there was no significant difference in the percentage of $CD4^+$ T cells between the two groups (**Figure 1F**). These results suggested that high-nitrate intake skews the splenic immune profile towards innate immunity, which was characterized by expansion of $CD11b^+F4/80^+$ macrophages and $CD11b^+Ly6G^+$ neutrophils concurrent with a reduction in adaptive T-cell frequency.

## NaD promotes gastric inflammation and disrupts mucosal barrier function

The mRNA expression of 84 cytokines and chemokines in the gastric mucosa of NaD-treated mice was analyzed to characterize the NaD-triggered inflammatory response (**Figure 2A**). NF-κB p65 expression, a master regulator of pro-inflammatory cytokines, was upregulated in the NaD-fed group (**Figure 2B**). qPCR validation demonstrated significant upregulation of Ccl20 ($P = 0.031$) and Cxcl5 ($P = 0.031$) after 1 week of NaD treatment (**Figure 2C**), whereas IL-17a ($P = 0.013$), Ccl20 ($P = 0.004$), IL-6 ($P = 0.018$), Cxcl5 ($P = 0.047$), and Ccl2 ($P = 0.0377$) were all upregulated in the 2-week NaD group (**Figure 2D**, **Figure S2**). Direct treatment of GES-1 cells with 40 mM sodium nitrate did not significantly alter mRNA expression of inflammatory cytokines (**Figure 2E**). This finding indicated that the metabolic processing of nitrate is likely microbiota-dependent. In addition, a modest upward trend in serum inflammatory markers was noted in NaD-treated mice (**Figure 2F**), suggesting a mild systemic response. An analysis of the gastric content pH revealed comparable levels (pH 5–6) in the ND and NaD mice (**Figure 2G**), suggesting that high-nitrate intake had no effect on gastric acidity. In addition, 2 weeks of NaD treatment impaired gastric mucosal barrier function, as evidenced by downregulation of

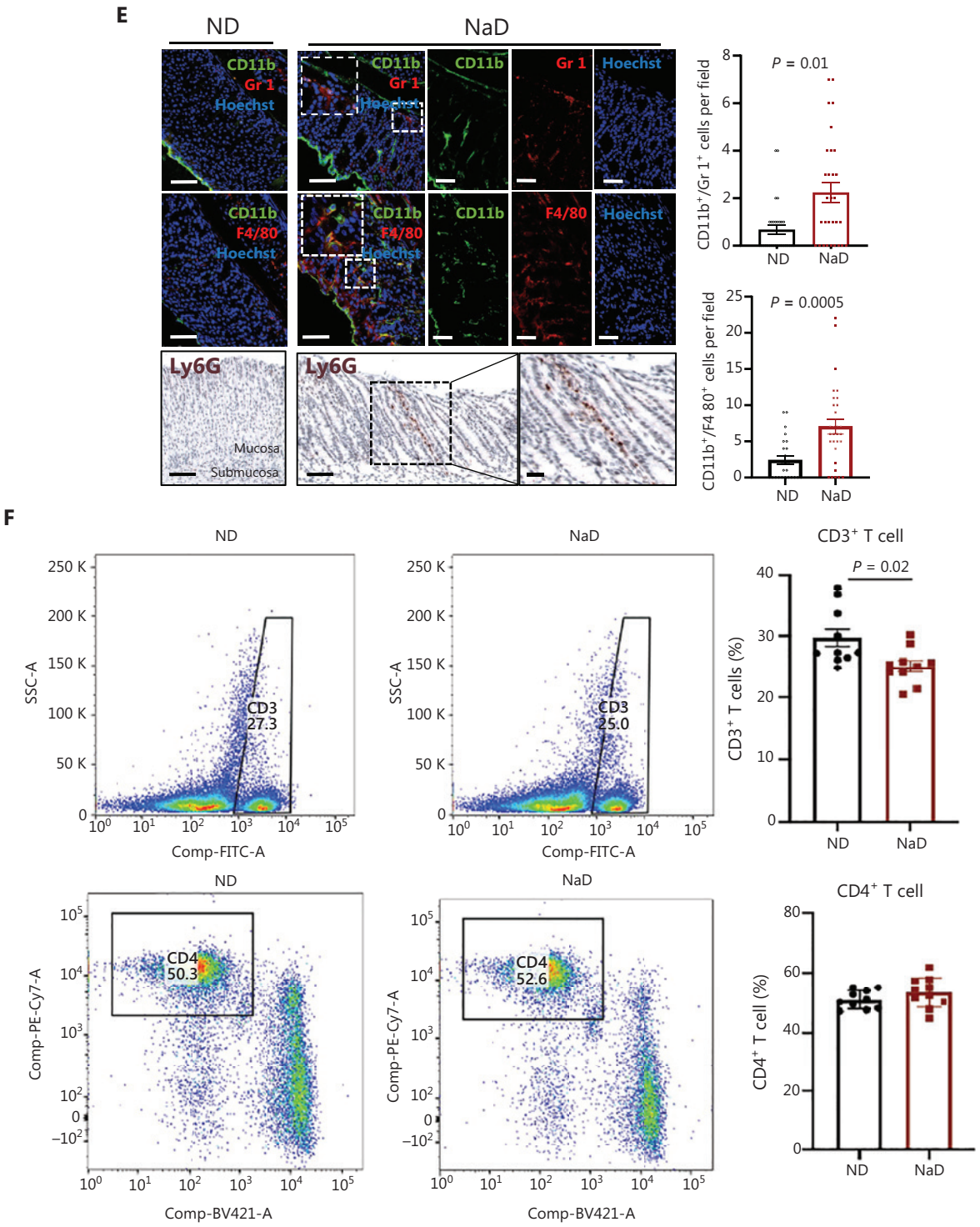



**Figure 1** NaD induces gastritis with infiltration of neutrophils and macrophages in C57BL/6 mice. (A) Study design scheme for conventional 7-week-old C57BL/6 mice fed an ND or NaD for 1 or 2 weeks. (B) Representative H&E staining images of gastric mucosa for a 1- and 2-week NaD, including focal inflammation, mild inflammation, and normal. Scale bars, 50μm. (C) Gastric mucosal pathologic scores for the ND ($n$ = 20), 1-week NaD ($n$ = 10), and 2-week NaD groups ($n$ = 10). Data are shown as the mean ± SEM. One-way ANOVA test was used to determine the statistical significance among groups. (D) Pathologic diagnosis statistics of gastric mucosa among ND ($n$ = 20), 1-week NaD ($n$ = 10), and 2-week NaD groups ($n$ = 10). (E) Representative IF and IHC images (captured 2-3 views for each mouse) of CD11b, Gr 1, F4/80, and Ly6G in

gastric mucosa between ND ($n$ = 10) and NaD ($n$ = 10). Scale bars, 50 μm. Data are shown as the mean ± SEM. Student's $t$-test was used to determine the statistical significance between groups. (F) Representative FACS plots and summary graphs of $CD3^+$ and $CD4^+$ T cells in ND- and NaD-treated mice ($n$ = 10 per group). The percentage of $CD3^+$ cells was significantly lower in the NaD group ($P$ = 0.02), while $CD4^+$ Cells levels were comparable between groups. Data are shown as the mean ± SEM. Student's $t$-test was used to determine the statistical significance between groups. Abbreviations: IF, immunofluorescence; IHC, immunohistochemistry; NaD, high-nitrate diet; ND, normal diet.

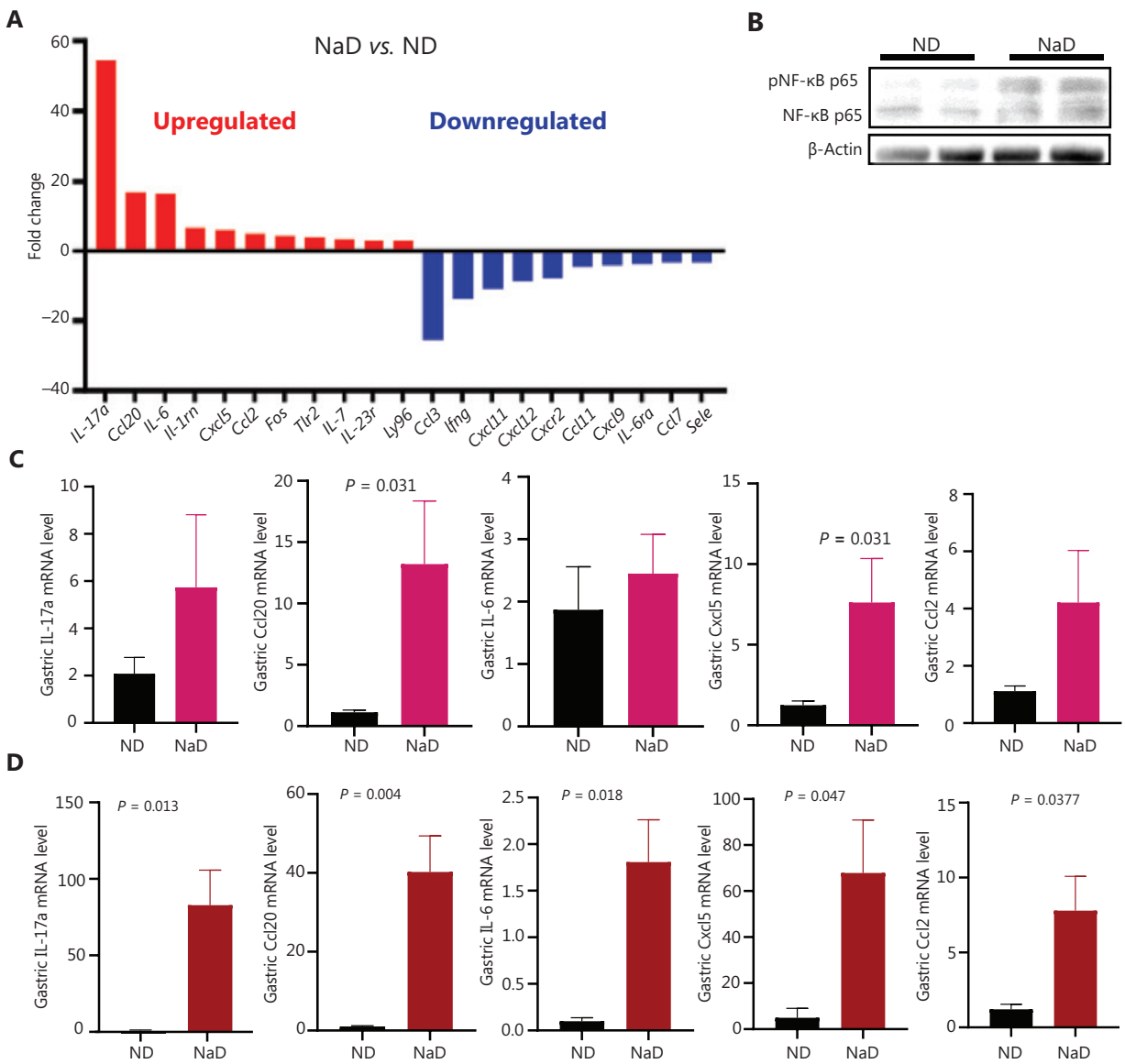



**Figure 2** Continued

key tight junction proteins (ZO-1, E-cadherin, and claudin-1; **Figure 2H**). IF staining showed reduced ZO-1 expression and a loss of continuous membrane localization (**Figure 2I**). These results indicated that NaD treatment elevated inflammatory chemokines and cytokines and impaired gastric mucosal barrier integrity.

## NaD induces taxonomic and functional shifts in the gut microbiota

To investigate whether dietary nitrate intake modulates the stomach and gastrointestinal tract microbiome, the microbial communities in gastric mucosa, gastric content, and

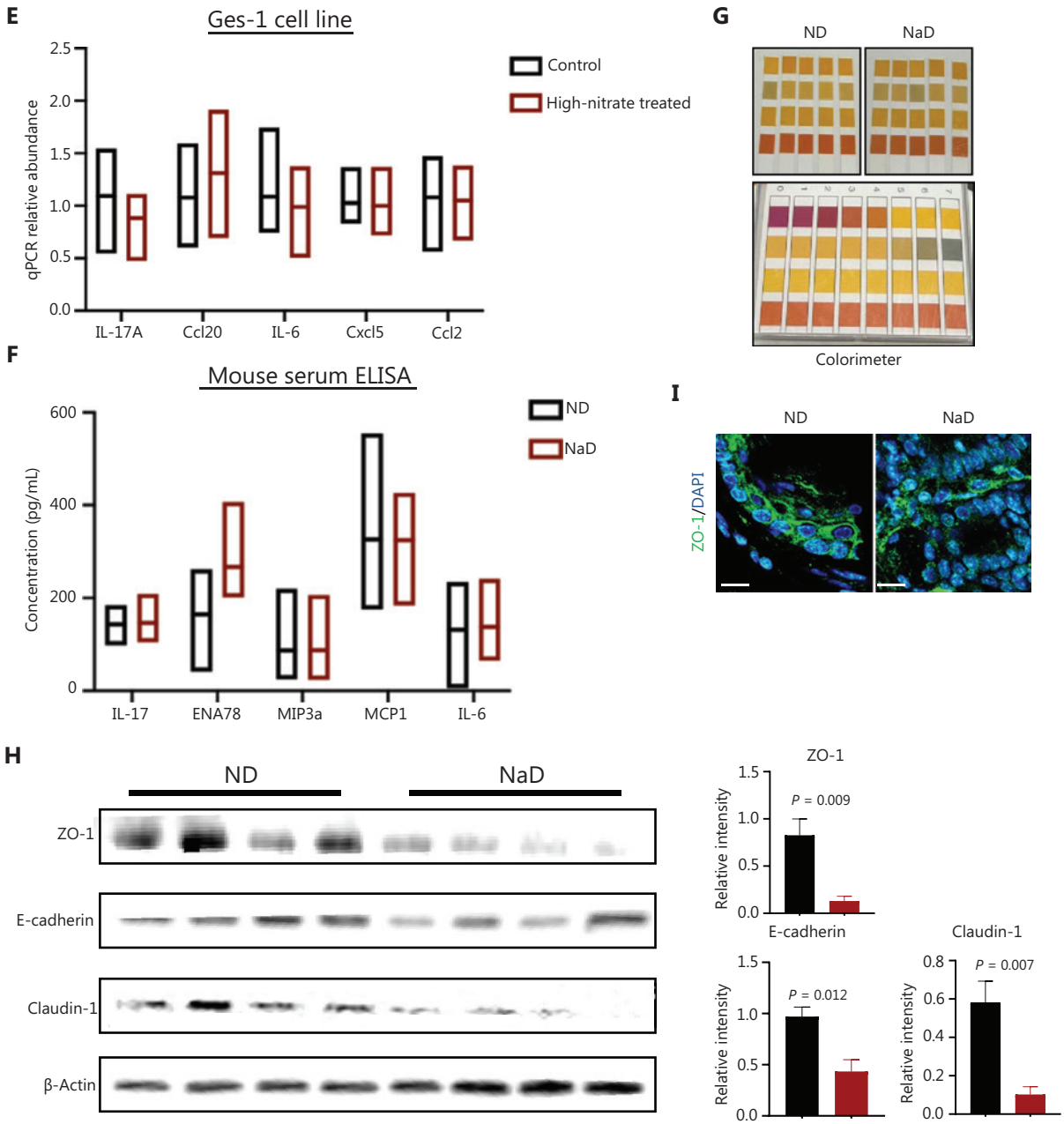



**Figure 2** NaD elevates inflammatory chemokines and cytokines and impairs gastric barrier. (A) Inflammatory response and autoimmunity PCR array under different treatments. (B) Western blot for NF-κB protein in gastric mucosa between the ND and NaD groups. (C) qPCR validation for increased expression of IL-17a, Ccl20, IL-6, Cxcl5, and Ccl2 after 1-week NaD treatment. Data are shown as the mean ± SEM. Student's *t*-test was used to determine the statistical significance between groups. (D) qPCR validation for increased expression of IL-17a, Ccl20, IL-6, Cxcl5, and Ccl2 after 2-week NaD treatment. Data are shown as the mean ± SEM. Student's *t*-test was used to determine the statistical significance between groups. (E) qPCR validation of the Ges-1 cell line after high-nitrate treatment (40 mM) for inflammatory cytokine expression (IL-17a, Ccl20, IL-6, Cxcl5, and Ccl2). Data are shown as the mean. Student's *t*-test was used to determine the statistical significance between groups. (F) ELISA for mouse serum inflammatory cytokines treated with NaD. Data are shown as the mean. Student's *t*-test was used to determine the statistical significance between groups. (G) Measurement of gastric pH. Representative images showing pH indicator strips used to test gastric contents from ND- and NaD-treated mice. The colorimetric reference scale is displayed at the bottom of the panel. (H) Western blot analysis of tight junction markers (ZO-1, E-cadherin, and claudin-1) were downregulated in the stomachs of NaD-fed mice. Data are shown as the mean ± SEM. Student's *t*-test was used to determine the statistical significance between groups. (I) Representative IF images of mouse gastric mucosa after exposure to NaD. Scale bars, 5 μm. Abbreviations: IF, immunofluorescence; NaD, high-nitrate diet; ND, normal diet.

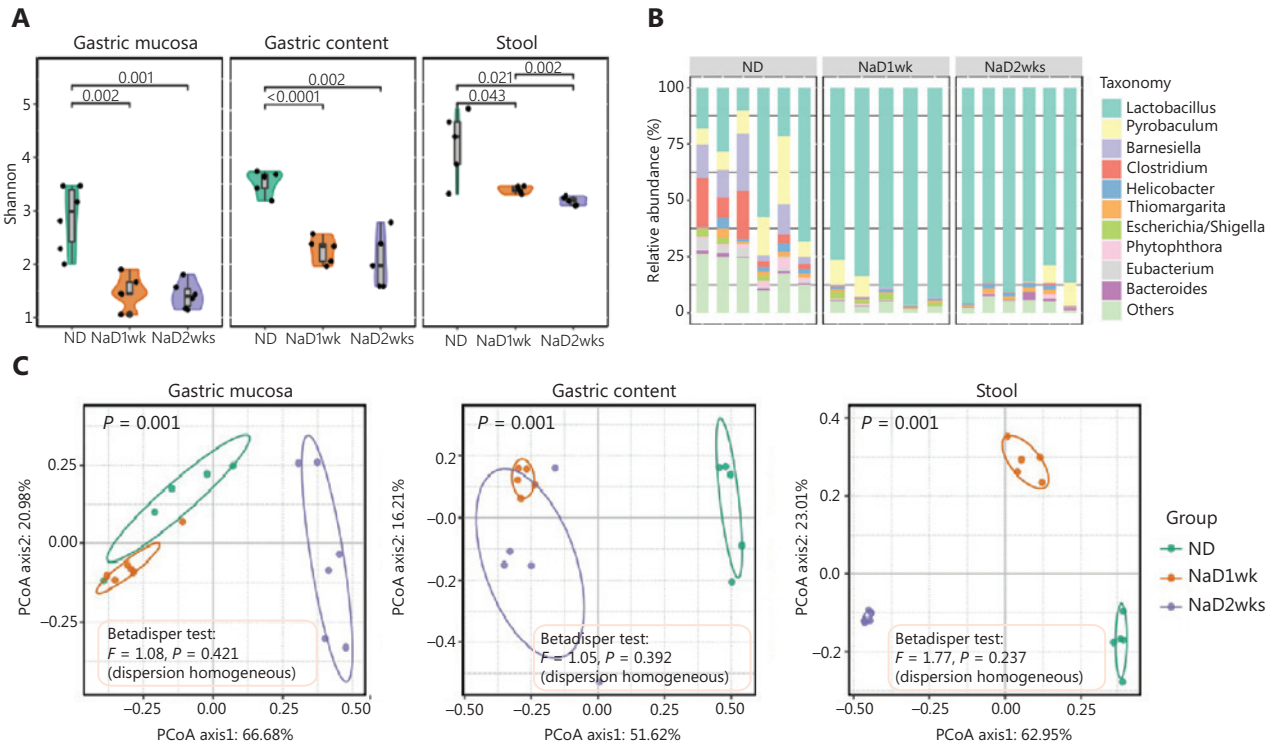



**Figure 3** Continued

stool sampled from NaD-treated and ND-fed mice were characterized. NaD intervention significantly reduced the Shannon diversity in gastric mucosa and gastric content after just 1 week, which persisted through the 2nd week and was consistently observed in stool samples (**Figure 3A**). Specifically, NaD treatment caused a dramatic microbial shift in the gastric mucosa dominated by *Lactobacillus*, which increased to > 75% of the total composition compared to controls (**Figures 3B and S3A**). This finding might be due to the ability of *Lactobacilli* to convert nitrate into NO and nitrite, allowing *Lactobacilli* to thrive. In addition, *Firmicutes* was enriched in gastric content and stool samples after NaD treatment (**Figure S3B and S3C**). Beta diversity analysis revealed a clear separation between NaD-treated mice and ND-fed mice in gastric mucosa, gastric content, and stool samples (**Figure 3C**), indicating that NaD induces ecologic disruption of the gastrointestinal tract microbiome. At the species level, potential pathogens, such as *E. gallinarum*, *Prevotella timonensis*, and *Mycobacterium gordonae*, were enriched in gastric mucosa after 2 weeks of NaD treatment (**Figure 3D**). Analysis of microbial gene function showed that NaD treatment induced enrichment of the nitrate reductase pathway in gastric content and stool samples (**Figure 3E**). Overlap of differential species among gastric mucosa, gastric content, and stool samples identified 3 commonly dysregulated species in the 1-week NaD group, which increased to 13 species in the 2-week NaD group (**Figure 3F**). *Roseburia hominis*, *Clostridium scindens*, and *Faecalibacterium prausnitzii*, all of which are probiotics, were the top 3 depleted species (**Figure 3G and 3H**). Collectively, these results demonstrated that NaD dietary intervention provoked microbial dysbiosis, which was marked by enrichment of potential pathogens in the gastric mucosa and concurrent depletion of probiotic bacteria in the gastrointestinal tract.

## NaD alters metabolism by upregulating the tryptophan pathway

The metabolic alterations induced by NaD treatment were characterized given the established role of microbiota-associated metabolites in health and disease. The metabolites in gastric mucosa, gastric content, serum, and stool samples were profiled and these data were integrated with metagenomic datasets. PLS-DA score plots revealed distinct metabolic clusters between NaD-treated and ND-fed controls across all sample types, including gastric mucosa (1- and 2-week NaD; **Figure 4A**), as well as gastric content, serum, and stool (**Figure 4B**). The concomitant metabolic alterations in the gastric mucosa were characterized given the observed enrichment of pathogenic species. Specifically, 56 metabolites were elevated and 20 were depleted after NaD treatment for 1 or 2 weeks (**Figure 4C and 4D**). KEGG

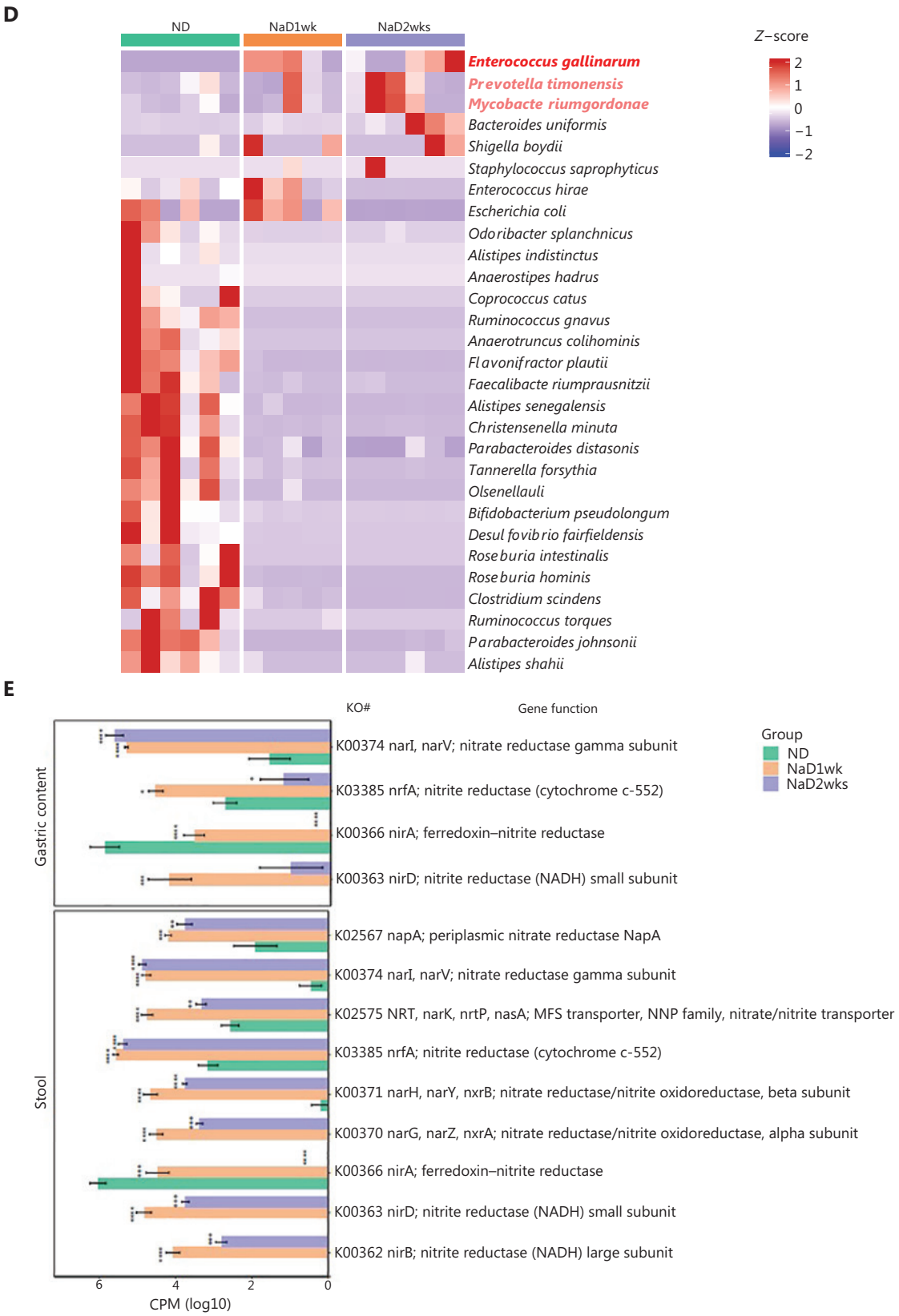



**Figure 3** Continued

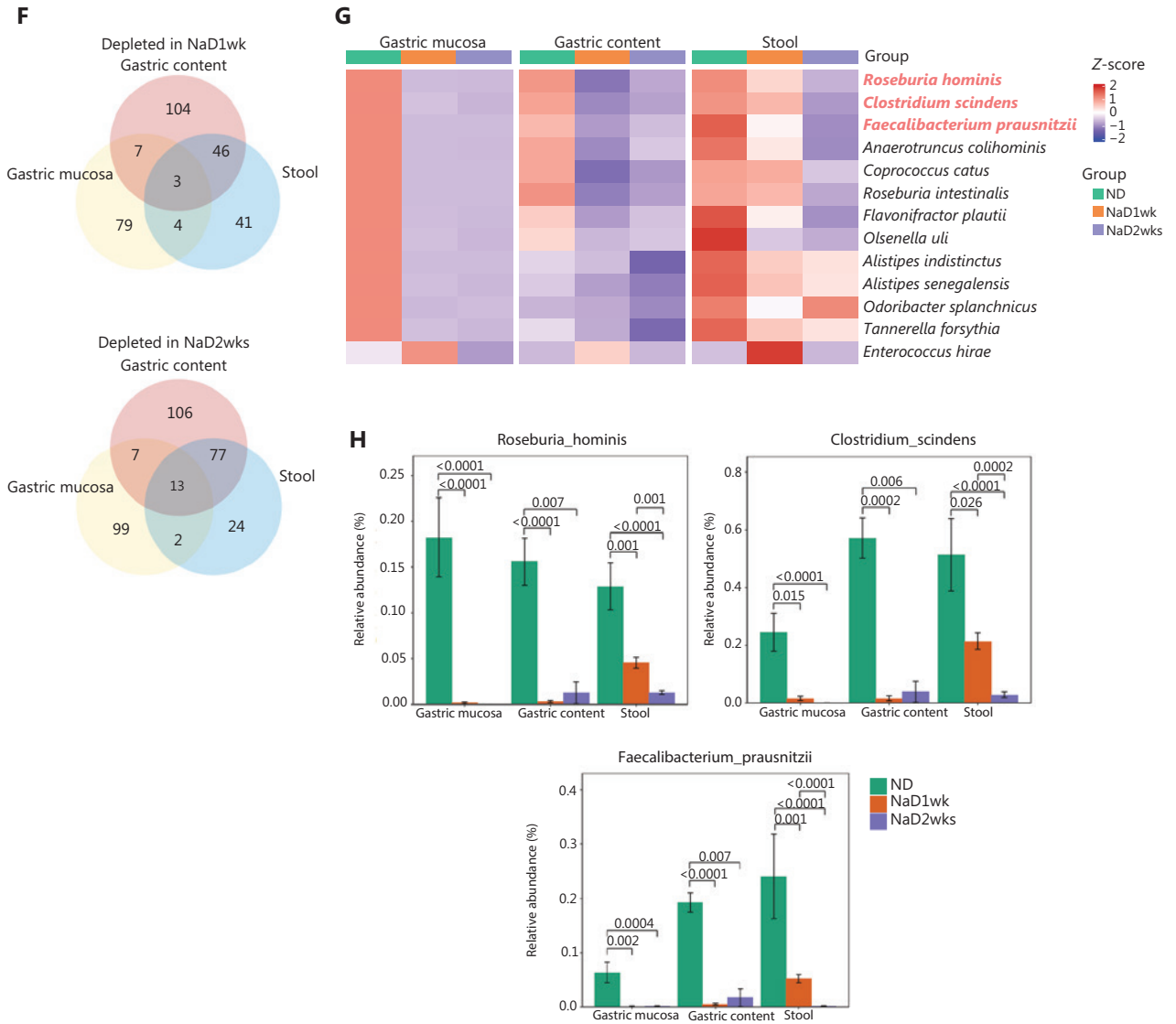



**Figure 3** Alterations of microbial and functional shift in multiple sites of the GI tract induced by NaD. (A) NaD significantly reduced microbial alpha diversity (Shannon index) in gastric mucosa, gastric content, and stool samples compared to ND. (B) Relative abundance of microbial composition in gastric mucosa following NaD *versus* ND feeding. (C) Beta diversity was calculated using PCoA based on the Bray–Curtis distance among different diet groups within the gastric mucosa, gastric content, and stool samples, respectively. Ellipses represent 95% confidence intervals; statistical significance was assessed using PERMANOVA. (D) Heatmap displaying differentially abundant species in gastric mucosa after 1- and 2-week NaD treatment compared to ND. Significance was determined by edgeR; the top three enriched species are highlighted in red. (E) Bar plot illustrating nitrate-related functional changes in gastric content and stool samples after 1- and 2-week NaD treatment relative to ND. *$P$ < 0.05, **$P$ < 0.01, ***$P$ < 0.001, and ****$P$ < 0.0001. (F) Venn diagrams depicting unique and overlapping depleted microbial species across gastrointestinal sites after 1- (upper) and 2-week (lower) NaD treatment compared to ND. (G) Heatmap visualizing the relative abundance of overlapping differentially abundant bacteria in gastric mucosa, gastric content, and stool samples. The top three depleted species are marked in red. (H) Bar plots comparing the abundance of *Roseburia hominis*, *Clostridium scindens*, and *Faecalibacterium prausnitzii* across gastric mucosa, gastric content, and stool samples after ND and NaD treatment. Abbreviations: NaD, high-nitrate diet; ND, normal diet; PCoA, principal coordinates analysis.

pathway enrichment analysis of these differentially expressed metabolites implied significant involvement of tryptophan-related metabolic pathways, including upregulation of tryptophan metabolism in the 1-week NaD group and enrichment of phenylalanine, tyrosine, and tryptophan biosynthesis in the 2-week NaD group (**Figure 4E**). Ten metabolites were consistently altered across both time points. Among the metabolites, 5-Hydroxyindoleacetate (5-HIAA) was the leading upregulated

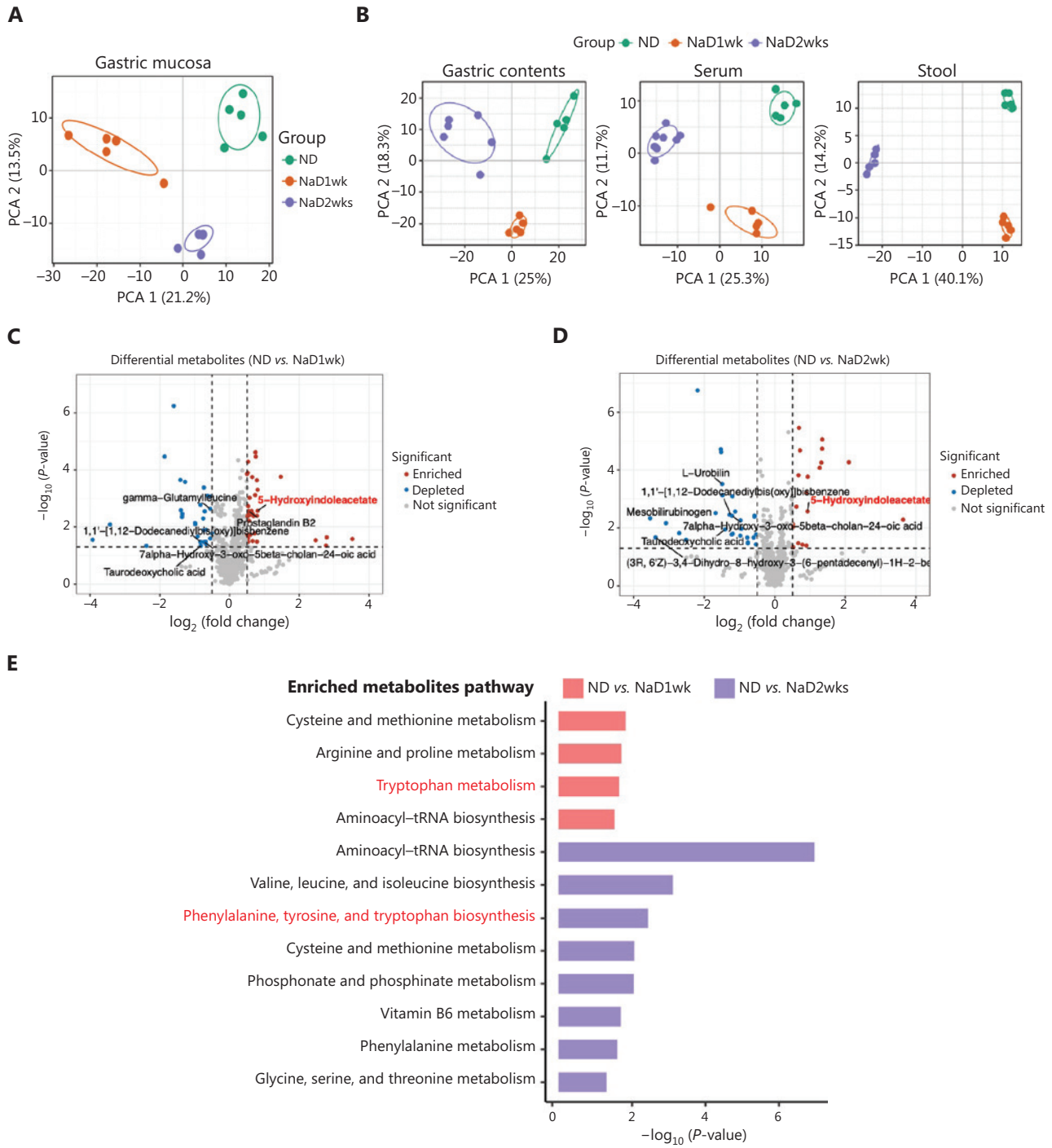



**Figure 4** Continued

metabolite (**Figure 4F**). Spearman correlation analysis was performed between the differentially expressed microbial species and tryptophan-related metabolites to correlate these findings with the gastric microbiome. This analysis revealed significant negative correlations of 5-HIAA and indole-3-carboxaldehyde with depleted probiotic species, including *R. hominis, C. scindens*, and *F. prausnitzii*. Additionally, indole lactic acid was negatively correlated with *R. hominis*, whereas 5-HIAA exhibited a positive correlation with *E. gallinarum*. (rho < −0.5, $P < 0.05$; **Figure 4G**). In summary, NaD alters tryptophan metabolism in the gastric mucosa, which is closely associated with concurrent microbial disturbance.

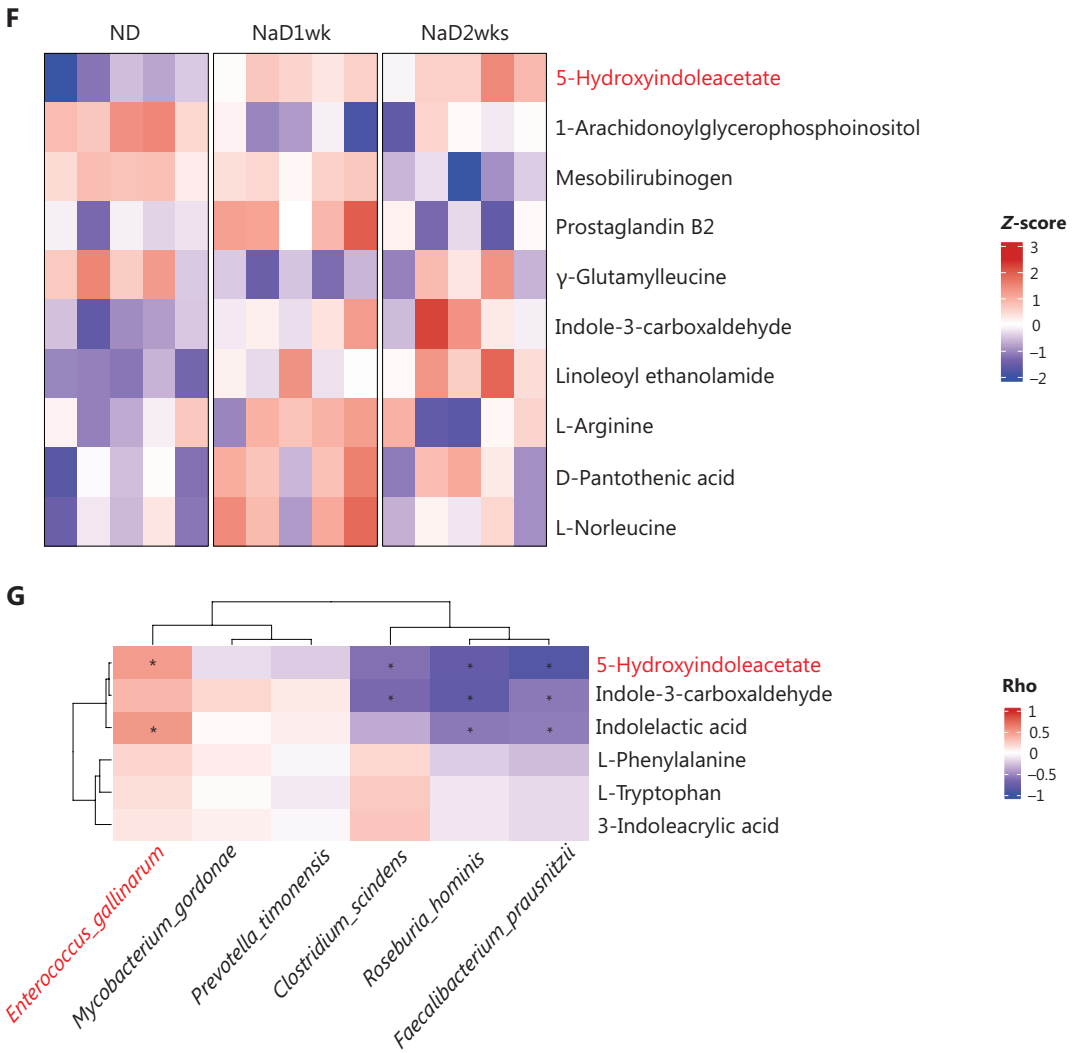



**Figure 4** Distinct metabolome profile after NaD treatment in gastric mucosa, gastric contents, serum, and stool samples. (A) PLS-DA score plots for gastric mucosa in different groups. X and Y axes represent contributions of persons to the first two principal components (PCA 1 and PCA 2). (B) PLS-DA score plots for gastric contents, serum, and stool samples in different groups. (C-D) Volcano plot showing fold-changes in metabolites between ND and 1-week NaD treatment (C) and between ND and 2-week NaD treatment (D) in gastric mucosa. Metabolites with a fold-change threshold ≥ 1.20 or ≤ 0.80 and a *P* value < 0.05 are identified as significant and represented by colored circles with enriched metabolites in red and depleted in blue. (E) Bar plot of metabolite enrichment analysis determined by the altered metabolites in gastric mucosa. The tryptophan-related pathway was colored in red. (F) Heatmap presented the differential metabolites among ND and 1- and 2-week NaD treatment in gastric mucosa with the top enriched metabolites marked in red. (G) Correlation heatmap identifying associations between differential microbial species and metabolites in gastric mucosa. The red color indicates a positive correlation, while the purple color shows a negative correlation. *$P$ < 0.05. Abbreviations: NaD, high-nitrate diet; ND, normal diet; PLS-DA, partial least square discriminant analysis.

## *E. gallinarum* or 5-HIAA treatment exacerbate gastritis in conventional and germ-free mouse models

Next, the functional role of NaD-associated pathogenic bacteria and metabolites in gastritis development were validated in a conventional mouse model (**Figure 5A**). Mice were gavaged with *E. gallinarum* ($1 \times 10^8$ CFU), 5-HIAA (5 mg/kg), or vehicle daily for 3 weeks. Stomach tissues were harvested and processed for HE staining (**Figure 5B**). Mice treated with *E. gallinarum* or 5-HIAA exhibited significantly increased pathologic scores (**Figure 5C**) and severe histologic diagnoses, characterized by varying degrees of inflammation with foci and clusters of neutrophil infiltration (**Figure 5D**). These

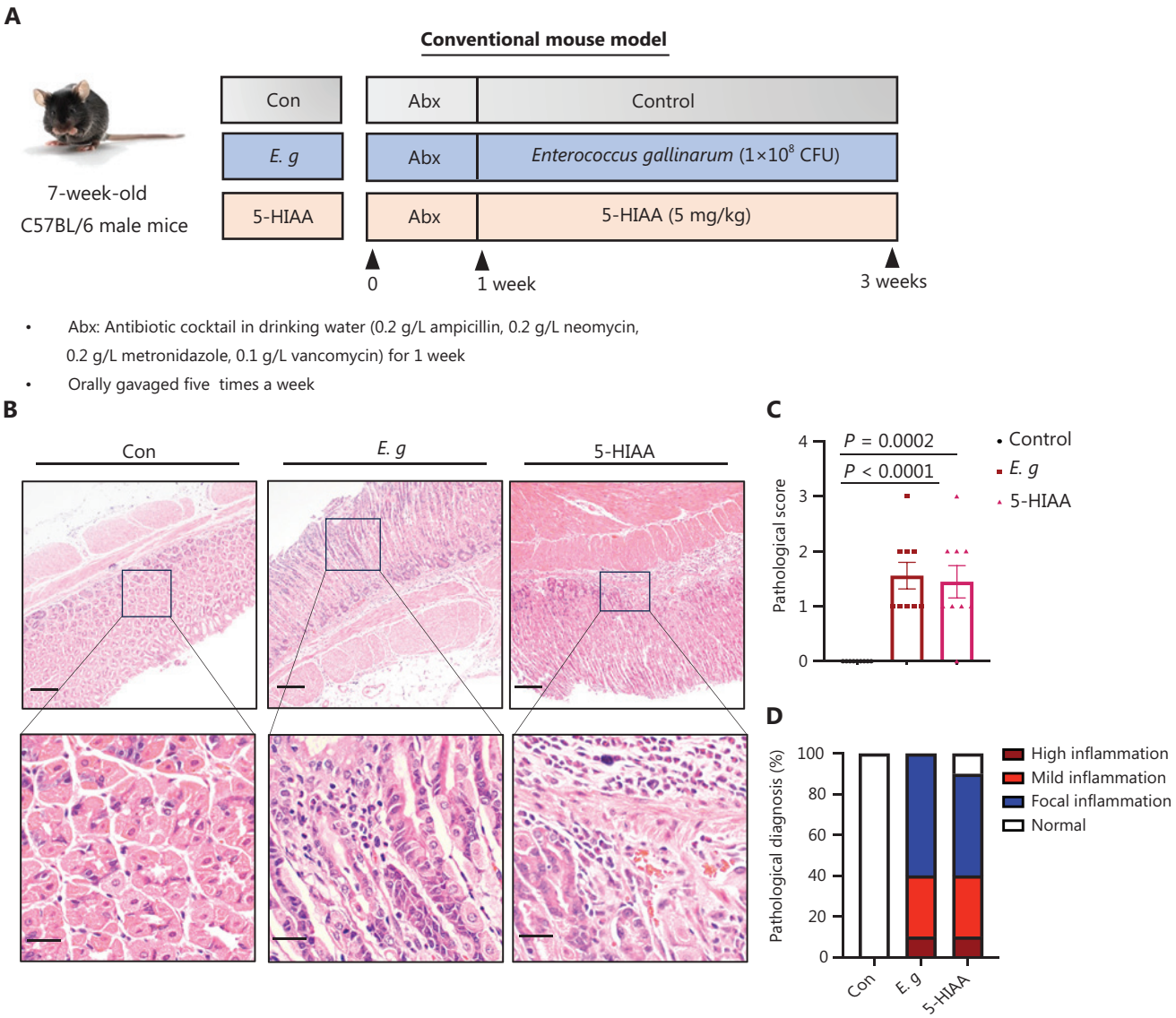



**Figure 5** Continued

treatments were then performed on an additional germ-free mouse model to validate that the phenotypic effects of *E. gallinarum* or 5-HIAA were independent of other components of the gut microbiota (**Figure 5E**). Histologic analysis of gastric samples revealed the same phenotype (**Figure 5F**) with the *E. gallinarum* and 5-HIAA groups showing significantly higher pathologic scores (**Figure 5G**) and inflammation (**Figure 5H**). Taken together, these results suggested that NaD-associated pathogenic bacteria and metabolites contribute to the development of gastritis.

We next asked if *E. gallinarum* and 5-HIAA promote gastric inflammation through the induction of pro-inflammatory cytokines. Indeed, *in vitro* treatment of a gastric cell line (Ges-1) with 5-HIAA triggered a marked upregulation of pro-inflammatory cytokines chemokines (IL-17a, Cxcl5, and IL-6) enriched in the IL-17a signaling pathway (**Figure 5I**). These findings were subsequently validated in germ-free mice using qPCR array, confirming that *E. gallinarum* and 5-HIAA altered the expression of key inflammatory cytokines and chemokines (IL-17a, Ccl2, Ccl20, Cxcl5, and IL-6; **Figure 5J and 5K**), thus confirming our hypothesis.

# Discussion

Environmental factors heavily influence the human microbiota and diet is arguably the most critical factor in defining the microbial landscape in the gastrointestinal tract[20]. However, the interplay between diet and the gastric microbiota has not been established. Herein NaD administration was

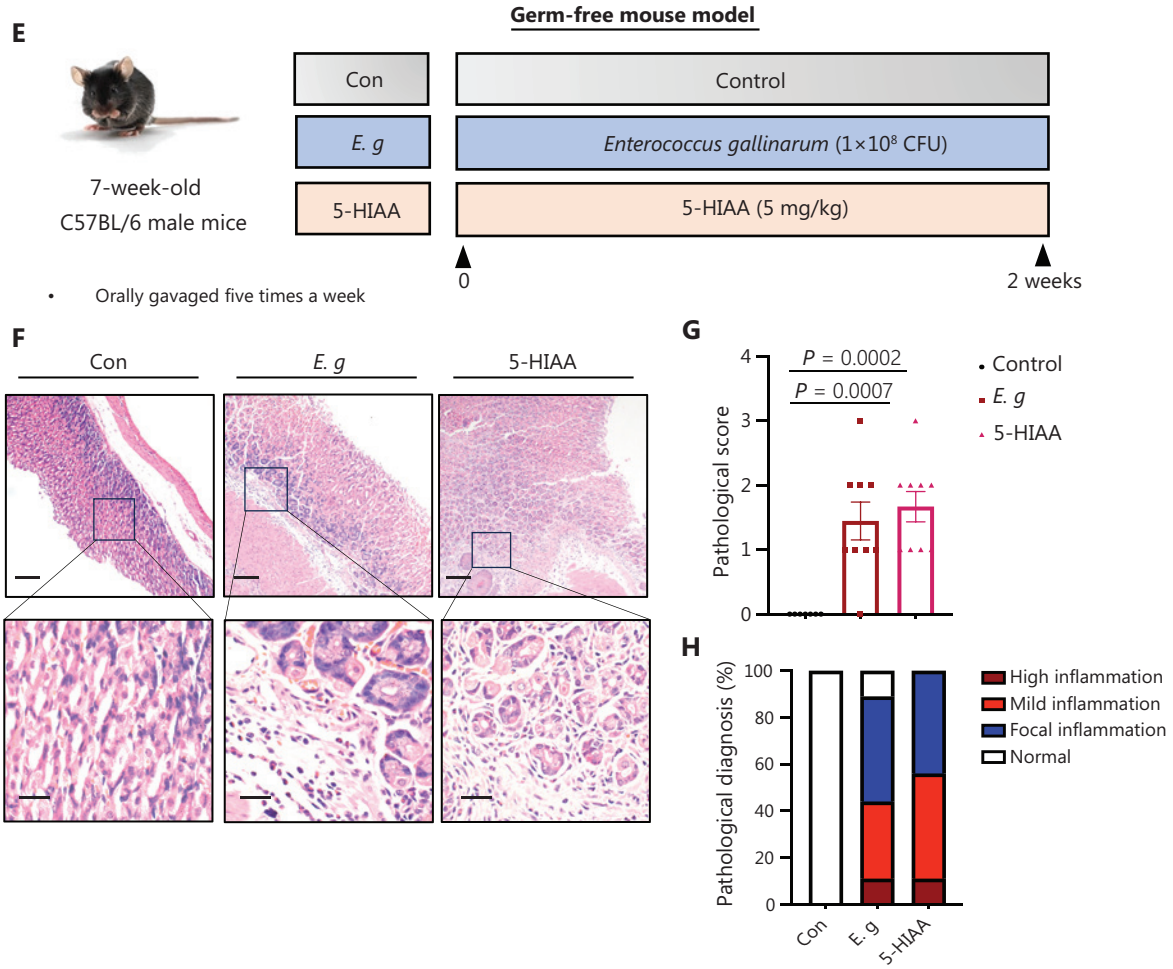



**Figure 5** Continued

shown to trigger gastritis with increased immune cell infiltration and pro-inflammatory cytokine levels. This finding was accompanied by the enrichment of pathogens and depletion of probiotics in the gastric mucosa. Integrative analyses identified the tryptophan metabolite, 5-HIAA, as enriched in NaD-induced gastritis and negatively correlated with probiotic abundance. Studies with an NaD-enriched pathogen (*E. gallinarum*) and metabolite (5-HIAA) in conventional and germ-free mice validated the contributory role in gastritis development. Collectively, the results inferred that NaD promotes gastritis by modulating the gastric microbiota and metabolites.

Epidemiologic evidence has suggested the ingestion of nitrate may be associated with an increased risk of developing gastric pathologies. This potential link has been proposed to occur through the formation of carcinogenic nitrosamine compounds that can promote tumorigenesis[21]. However, how NaD elicits gastritis is far from understood. Herein a diet supplemented with 7.5% NaD was shown to be associated with gastritis and severe inflammation in mice. It is important to acknowledge that the 7.5% sodium nitrate concentration used in this study represents a supra-physiologic dietary intervention. This allows for the mechanistic dissection of nitrate-driven inflammatory pathways and dysbiosis, distinct from chronic low-dose dietary exposure. The findings revealed that NaD intake triggers a pro-inflammatory state in the gastric mucosa that is characterized by the presence of infiltrating inflammatory cells, including neutrophils and macrophages. NaD also strongly activated chemokines and cytokines signaling pathway in the gastric mucosa, particularly IL-17a, Ccl20, IL-6, Cxcl5, and Ccl2, concurrent with activation of NF-κB. Chemokines and cytokines are key signaling molecules that orchestrate trafficking of immune cells[22] and are likely mediators of the pro-inflammatory state. Furthermore, NaD dietary intervention compromised the gastric mucosal barrier, as indicated by downregulation of critical tight junction proteins

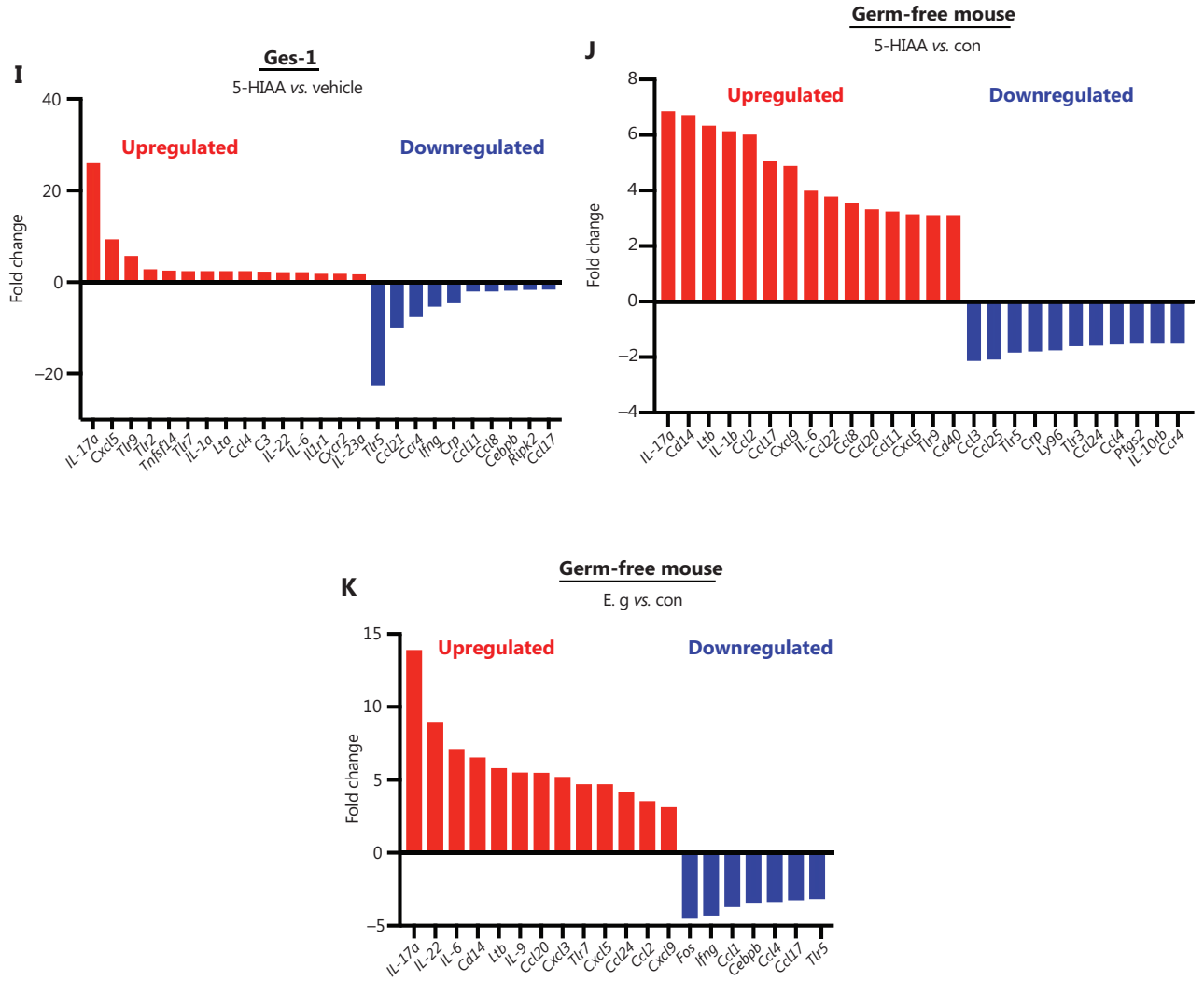



**Figure 5** Treatment with *E. gallinarum* or 5-HIAA exacerbated the gastritis. (A) Schematic diagram of the experimental design for the conventional mouse model ($n$ = 10 mice per group). (B) Representative H&E staining images of stomach mucosa for control, *E. gallinarum*, or 5-HIAA treatment in the conventional mouse model. Scale bars: 200 μm for the upper panel (10× objective), 50 μm for the lower panel (40× objective). (C) Pathologic score of stomach mucosa for the control, *E. gallinarum*, or 5-HIAA treatment in the conventional mouse model. (D) Pathologic diagnosis statistic of stomach mucosa for control, *E. gallinarum*, or 5-HIAA treatment in the conventional mouse model. (E) Schematic diagram of the experimental design for the conventional mouse model (control: $n$ = 8; *E. gallinarum*: $n$ = 9; 5-HIAA: $n$ = 9). (F) Representative H&E staining images of stomach mucosa for control, *E. gallinarum*, or 5-HIAA treatment in the germ-free mouse model. Scale bars: 200 μm for the upper panel (10× objective), 50 μm for the lower panel (40× objective). (G) Pathologic score of stomach mucosa for the control, *E. gallinarum*, or 5-HIAA treatment in the germ-free mouse model. (H) Pathologic diagnosis statistic of stomach mucosa for control, *E. gallinarum*, or 5-HIAA treatment in the germ-free mouse model. (I) Inflammatory response and autoimmunity PCR array using 5-HIAA treatment for the Ges-1 cell line. (J) Inflammatory response and autoimmunity PCR array using 5-HIAA treatment in the germ-free mouse model. (K) Inflammatory response and autoimmunity PCR array using *E. gallinarum* treatment in the germ-free mouse model. Abbreviations: 5-HIAA, 5-hydroxyindoleacetate; *E. gallinarum, Enterococcus gallinarum*.

(ZO-1, E-cadherin, and claudin-1). Taken together, NaD administration was shown to induced a series of pathologic changes leading to gastritis with overt inflammation and a loss of barrier integrity. Long-term exposure to NaD might thus lead to chronic gastritis and an increase in the risk of gastric tumorigenesis.

Accumulating evidence has demonstrated that the gut microbiome is closely associated with tumor initiation and

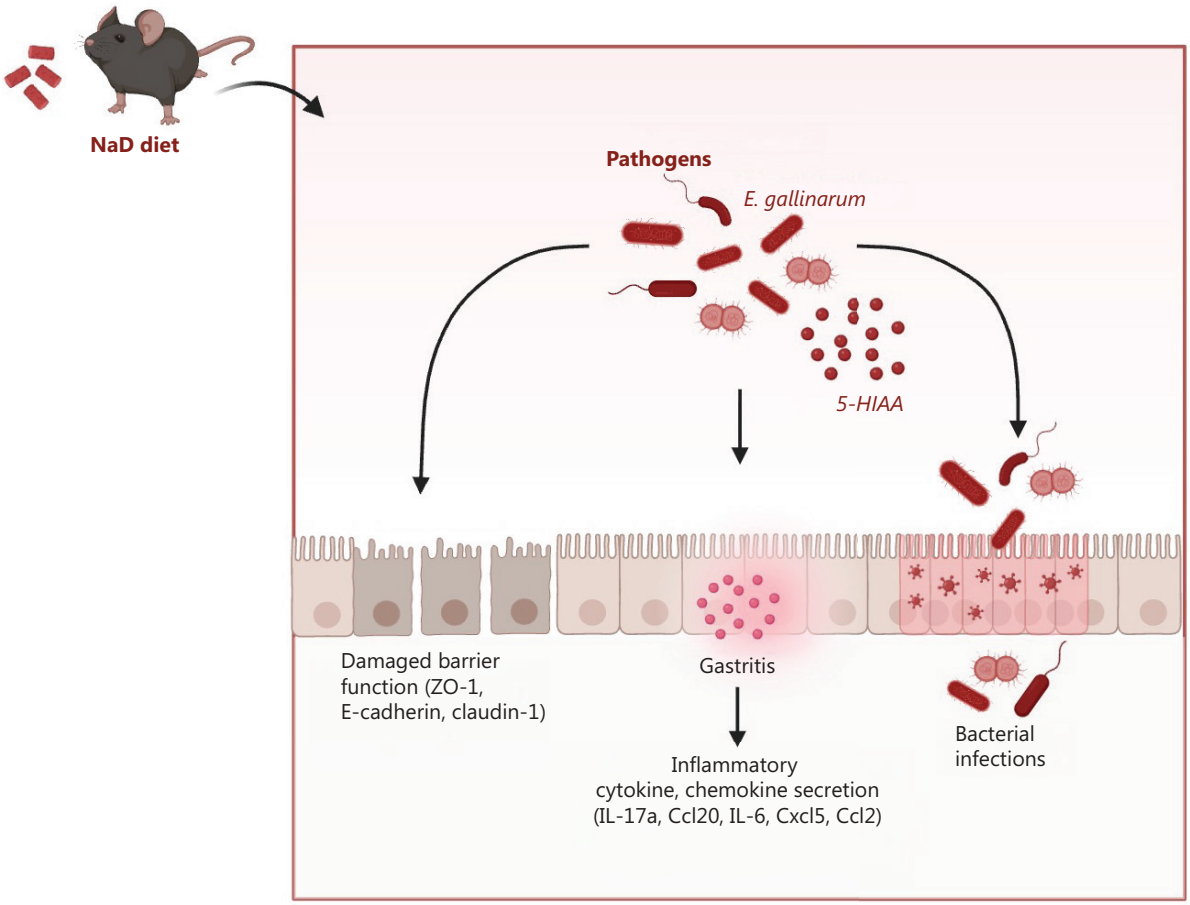



**Figure 6** Schematic illustration links a NaD to gastritis in a mouse model. NaD intake induces significant gastric dysbiosis, characterized by enrichment of the pathogenic bacterium, *E. gallinarum*, and depletion of beneficial species. This microbial shift is accompanied by metabolic reprogramming, specifically the upregulation of tryptophan metabolism and the accumulation of 5-HIAA. Mechanistically, both *E. gallinarum* colonization and elevated 5-HIAA act as pro-inflammatory triggers that stimulate the expression of cytokines and chemokines (including *IL-17a, Cxcl5, Il-6, Ccl20,* and *Ccl2*) in the gastric mucosa. This inflammatory signaling promotes the infiltration of innate immune cells, specifically $CD11b^{+}F4/80^{+}$ macrophages and $CD11b^{+}Ly6G^{+}$ neutrophils, while disrupting mucosal barrier integrity (e.g., downregulation of ZO-1), ultimately leading to the pathologic development of gastritis. Abbreviations: 5-HIAA, 5-hydroxyindoleacetate; *E. gallinarum, Enterococcus gallinarum*; NaD, NaD, high-nitrate diet.

progression in multiple solid tumors, including gastric cancer[23]. Our previous study revealed *S. anginosus* as a novel pathogen that promotes gastric tumorigenesis *via* direct interactions with gastric epithelial cells in the TMPC-ANXA2-MAPK axis[13]. To ask if NaD-induced gastritis involves alterations of the microbiome, comprehensive profiling of microbial communities was performed from gastric mucosa, gastric content, and stool samples. NaD feeding for 2 weeks significantly altered the gastric microbiota composition, characterized by an enrichment of pathogenic species (*E. gallinarum*, *P. timonensis*, and *M. gordonae*) and the depletion of beneficial species (*R. hominis*, *C. scindens*, and *F. prausnitzii*). Taken together, these data indicated that NaD induces a state of gastric dysbiosis, which potentially contributes to gastritis and disease pathogenesis.

The complex microbial communities inhabiting the gastrointestinal tract produce a vast array of small molecules and metabolites that interact with the host and play influential roles in regulating multiple physiologic processes, including metabolism, immune function, inflammation, and neurological processes[24-28]. Metabolomic analysis revealed that tryptophan metabolism is the top dysregulated metabolic pathway in NaD-treated mice. The correlation between the metagenome and metabolome were investigated given the important role of gut microbial metabolites in disease. A correlation analysis linked the changes

in tryptophan-related metabolites to key bacterial species altered by a NaD. Subsequent experiments confirmed that gavage with *E. gallinarum* and 5-HIAA was sufficient to recapitulate the gastritis phenotype, identifying *E. gallinarum* and the associated metabolite, 5-HIAA, as inflammation-promoting factors in the gastric mucosa.

## Conclusions

In summary, the current study elucidates a new pathogenic mechanism by which dietary nitrate promotes gastritis by modulating gastric microbiota and metabolites. NaD consumption initiates a cycle of inflammation and barrier dysfunction driven by gastric microbiome dysbiosis and associated metabolic shifts, including enrichment of *E. gallinarum* and the pro-inflammatory metabolite, 5-HIAA. This work provides a comprehensive framework linking environmental nitrate intake to gastric pathology *via* a host-microbe-metabolite axis.

## Grant support

This study was supported by the Noncommunicable Chronic Diseases-National Science and Technology Major Project (Grant No. 2023ZD0501400), the National Natural Science Foundation of China (Grant No. 82472896), the Strategic Seed Funding Collaboration Research Scheme CUHK (Grant No. 3133344), the Strategic Impact Enhancement Fund CUHK (Grant No. 3135509), and the Impact Case for RAE CUHK (Grant No. 3134277).

## Conflict of interest statement

No potential conflicts of interest are disclosed.

## Author contributions

Conceived and designed the analysis: Jun Yu, Lanping Jiang, Yongzhan Nie, Qing Li.
Collected the data: Lanping Jiang, Tianhui Li, Jiayu Wu, Xingyu Zhou, Alvin Ho Kwan Cheung, Qinyao Wei, Jing Ren.
Contributed data or analysis tools: Lanping Jiang, Tianhui Li.
Performed the analysis: Lanping Jiang, Tianhui Li.
Wrote the paper: Jun Yu, Lanping Jiang, Harry Cheuk-Hay Lau, Chi Chun Wong.

## Data availability statement

The data generated in this study are available upon request from the corresponding author.

## References

1. Sipponen P, Maaroos HI. Chronic gastritis. Scand J Gastroenterol. 2015; 50: 657-67.
2. Arita S, Inagaki-Ohara K. High-fat-diet-induced modulations of leptin signaling and gastric microbiota drive precancerous lesions in the stomach. Nutrition. 2019; 67-68: 110556.
3. Smyth EC, Nilsson M, Grabsch HI, van Grieken NC, Lordick F. Gastric cancer. Lancet. 2020; 396: 635-48.
4. Nitrate and human cancer. Lancet. 1977; 2: 281-2.
5. Jiang L, Lau HC, Zeng R, Yu J. Diet, Gastric Microbiota, and metabolites in gastric tumorigenesis. Research (Wash D C). 2025; 8: 0693.
6. Chazelas E, Pierre F, Druesne-Pecollo N, Esseddik Y, Szabo de Edelenyi F, Agaesse C, et al. Nitrites and nitrates from food additives and natural sources and cancer risk: results from the NutriNet-Santé cohort. Int J Epidemiol. 2022; 51: 1106-19.
7. Habermeyer M, Roth A, Guth S, Diel P, Engel KH, Epe B, et al. Nitrate and nitrite in the diet: how to assess their benefit and risk for human health. Mol Nutr Food Res. 2015; 59: 106-28.
8. Nardone G, Compare D. The human gastric microbiota: is it time to rethink the pathogenesis of stomach diseases? United European Gastroenterol J. 2015; 3: 255-60.
9. Clemente JC, Ursell LK, Parfrey LW, Knight R. The impact of the gut microbiota on human health: an integrative view. Cell. 2012; 148: 1258-70.
10. Yamashiro Y. Gut microbiota in health and disease. Ann Nutr Metab. 2017; 71: 242-46.
11. Carding S, Verbeke K, Vipond DT, Corfe BM, Owen LJ. Dysbiosis of the gut microbiota in disease. Microb Ecol Health Dis. 2015; 26: 26191.
12. Coker OO, Dai Z, Nie Y, Zhao G, Cao L, Nakatsu G, et al. Mucosal microbiome dysbiosis in gastric carcinogenesis. Gut. 2018; 67: 1024-32.
13. Fu K, Cheung AHK, Wong CC, Liu W, Zhou Y, Wang F, et al. *Streptococcus anginosus* promotes gastric inflammation, atrophy, and tumorigenesis in mice. Cell. 2024; 187: 882-96.e17.
14. Aviles-Jimenez F, Vazquez-Jimenez F, Medrano-Guzman R, Mantilla A, Torres J. Stomach microbiota composition varies between patients with non-atrophic gastritis and patients with intestinal type of gastric cancer. Sci Rep. 2014; 4: 4202.
15. Wang LL, Yu XJ, Zhan SH, Jia SJ, Tian ZB, Dong QJ. Participation of microbiota in the development of gastric cancer. World J Gastroenterol. 2014; 20: 4948-52.
16. Ferreira RM, Pereira-Marques J, Pinto-Ribeiro I, Costa JL, Carneiro F, Machado JC, et al. Gastric microbial community

profiling reveals a dysbiotic cancer-associated microbiota. Gut. 2018; 67: 226-36.
17. Kim KA, Gu W, Lee IA, Joh EH, Kim DH. High fat diet-induced gut microbiota exacerbates inflammation and obesity in mice via the TLR4 signaling pathway. PLoS One. 2012; 7: e47713.
18. Moreira APB, Texeira TFS, Ferreira AB, Peluzio Mdo C, Alfenas Rde C. Influence of a high-fat diet on gut microbiota, intestinal permeability and metabolic endotoxaemia. Br J Nutr. 2012; 108: 801-9.
19. Carmody RN, Gerber GK, Luevano JM Jr, Gatti DM, Somes L, Svenson KL, et al. Diet dominates host genotype in shaping the murine gut microbiota. Cell Host Microbe. 2015; 17: 72-84.
20. Zmora N, Suez J, Elinav E. You are what you eat: diet, health and the gut microbiota. Nat Rev Gastroenterol Hepatol. 2019; 16: 35-56.
21. Jensen OM. Nitrate in drinking water and cancer in northern Jutland, Denmark, with special reference to stomach cancer. Ecotoxicol Environ Saf. 1982; 6: 258-67.
22. Soloski MJ, Crowder LA, Lahey LJ, Wagner CA, Robinson WH, Aucott JN. Serum inflammatory mediators as markers of human Lyme disease activity. PLoS One. 2014; 9: e93243.
23. Peng R, Liu S, You W, Huang Y, Hu C, Gao Y, et al. Gastric microbiome alterations are associated with decreased $CD8^+$ tissue-resident memory T cells in the tumor microenvironment of gastric cancer. Cancer Immunol Res. 2022; 10: 1224-40.
24. Lu Y, Yuan X, Wang M, He Z, Li H, Wang J, et al. Gut microbiota influence immunotherapy responses: mechanisms and therapeutic strategies. J Hematol Oncol. 2022; 15: 47.
25. Jugder BE, Kamareddine L, Watnick PI. Microbiota-derived acetate activates intestinal innate immunity via the Tip60 histone acetyltransferase complex. Immunity. 2021; 54: 1683-97.e3.
26. Zheng D, Liwinski T, Elinav E. Interaction between microbiota and immunity in health and disease. Cell Res. 2020; 30: 492-506.
27. Miyauchi E, Kim SW, Suda W, Kawasumi M, Onawa S, Taguchi-Atarashi N, et al. Gut microorganisms act together to exacerbate inflammation in spinal cords. Nature. 2020; 585: 102-6.
28. Erny D, Dokalis N, Mezo C, Castoldi A, Mossad O, Staszewski O, et al. Microbiota-derived acetate enables the metabolic fitness of the brain innate immune system during health and disease. Cell Metab. 2021; 33: 2260-76.e7.

**Cite this article as:** Jiang L, Li T, Wu J, Lau HCH, Wong CC, Zhou X, et al. Dietary nitrate drives gastritis by modulating gastric microbiota and metabolites. Cancer Biol Med. 2026; 23: 717-736. doi: 10.20892/j.issn.2095-3941.2025.0679